Aalborg Universitet

AALBORG UNIVERSITY

DENMARK

Minimizing the Levelized Cost of Energy in Single-Phase Photovoltaic Systems with an Absolute Active Power Control

Yang, Yongheng; Koutroulis, Eftichios; Sangwongwanich, Ariya; Blaabjerg, Frede

Link to publication from Aalborg University

Minimizing the Levelized Cost of Energy in Single-Phase Photovoltaic Systems with an Absolute Active Power Control

Yongheng Yang, *Member, IEEE*, Eftichios Koutroulis, *Senior Member, IEEE*, Ariya Sangwongwanich, and Frede Blaabjerg, *Fellow, IEEE*

Abstract— **Countries with considerable PhotoVoltaic (PV) installations are facing a challenge of overloading their power grid during peak-power production hours if the power infrastructure remains the same. To address this, regulations have been imposed on PV systems, where more active power control should be flexibly performed. As an advanced control strategy, the Absolute Active Power Control (AAPC) can effectively solve the overloading issues by limiting the maximum possible PV power to a certain level (i.e., the power limitation), and also benefit the inverter reliability due to the reduction in the thermal loading of the power devices. However, its feasibility is challenged by the associated energy losses. An increase of the inverter lifetime and a reduction of the energy yield can alter the cost of energy, demanding an optimization of the power limitation. Therefore, aiming at minimizing the Levelized Cost Of Energy (LCOE), the power limit is optimized for the AAPC strategy in this paper. The optimization method is demonstrated on a 3-kW single-phase PV system considering a real-field mission profile (i.e., solar irradiance and ambient temperature). The optimization results have revealed that superior performance in terms of LCOE and energy production can be obtained by enabling the AAPC strategy, compared to the conventional PV inverter operating only in the maximum power point tracking mode. In the presented case study, the minimum of the LCOE is achieved for the PV system when the power limit is optimized to a certain level of the designed maximum feed-in power (i.e., 3-kW). In addition, the LCOE-based analysis method can be used in the design of PV inverters considering long-term mission profiles.**

Index Terms— **Levelized cost of energy (LCOE); absolute active power control; constant power generation control; reliability; single-phase photovoltaic (PV) systems**

I. INTRODUCTION

Solar PhotoVoltaic (PV) installations are still at a spectacular growth rate worldwide [1], and thus challenging issues

like overloading of the distributed grid due to peak power generation of PV systems appear occasionally [2]–[4]. In the case of a large-scale adoption of PV systems, advanced control strategies, e.g., power-ramp control and absolute power control, which are currently required for wind power systems in different countries, have also been strengthened into PV systems [3]–[12]. Referring to the Absolute Active Power Control (AAPC) in the Danish grid code [7], a constant power generation control concept for PV systems by limiting the maximum feed-in power has been proposed in [6] in order to solve the overloading issues in peak-power production periods, while other methods have also been developed in literature. However, either increased total cost or control complexity has been observed in the prior-art solutions. For instance, expanding the grid capacity (i.e., grid reinforcement) will incur additional investments, and integrating energy storage systems to tolerate the peak power not only increases the control complexity but also lowers the entire system reliability [13]–[15]. In contrast, the AAPC scheme requires only minor software modifications when implemented, being a feasible and cost-effective strategy [12], [14]–[19]. This explains why such a power control is gaining much awareness in some countries like Germany, Denmark, and Japan [7], [9], [11].

In addition, the AAPC feasibility in grid-connected PV applications has been investigated in [6] and [14] in terms of a rough estimation of the energy losses and also the PV inverter lifetime, respectively, where the AAPC scheme is also referred to as a Constant Power Generation (CPG) control. First, it has been found that the AAPC scheme with a reasonable power limitation (e.g., 80%) would not annually result in a substantial energy yield reduction [3], [6]. Furthermore, as a consequence of applying the AAPC strategy, a reduction of the thermal stresses on the power devices (e.g., Insulated-Gate Bipolar Transistor – IGBTs) has been achieved, since the power losses inducing temperature rises will be changed, when the PV system enters into the AAPC mode from the Maximum Power Point Tracking (MPPT) mode and also reversely. Therefore, a hybrid control method (MPPT-AAPC) will also contribute to improved reliability and thereby extended lifetime of the PV system beyond resolving the overloading issues [6], [14].

Notably, both the energy production and the system lifetime are main indicators of the Levelized Cost Of Energy (LCOE), which has become the key to increase the competitiveness of the PV systems with other renewables [20]–[22]. Thus, many efforts have been devoted into the design and control of PV systems with a common goal to reduce the cost of energy (i.e., lower LCOE) [23]–[25]. For instance, a circuit-
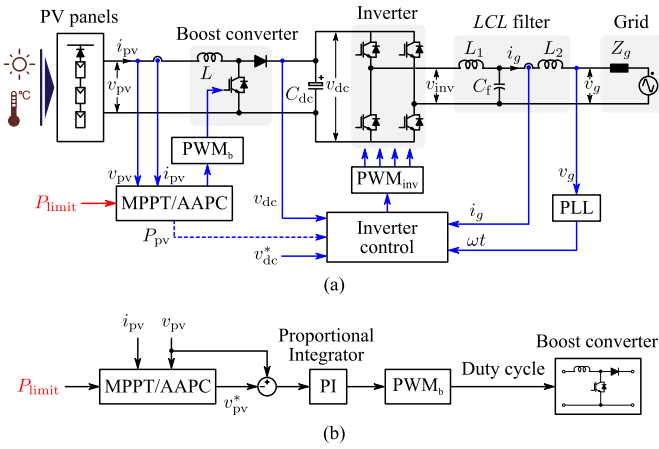
Fig. 1.   A single-phase double-stage grid-connected PV system with an *LCL* filter: (a) hardware schematic and overall control structure and (b) control block diagram of the boost converter with the Absolute Active Power Control (AAPC) scheme.

Fig. 2.   Power-voltage characteristic of a PV array (solar irradiance: 1000 W/m^2; ambient temperature: 25 °C), where the power limit of 80 % of the rated power (i.e., P_{limit} = 2.4 kW) is also shown.

level design of a PV inverter considering the failure rate of the circuit devices (calculated according to [26]) has been presented in [22]. Furthermore, means like adopting highly efficient transformerless PV inverters and reliability-oriented design have been witnessed in recent applications [22]–[24], [27]–[32]. An adoption of the transformerless PV inverters can somehow increase the energy production due to their high efficiency [28], [32], [33]. However, the MPPT-AAPC operational mode is against the objective of maximizing the energy production of the PV systems, although the "capped" energy is quite limited throughout a year [3], [6]. Whilst the improved reliability (i.e., extended service time of the PV systems) can compensate for such a loss to some extent as long as the power limitation is appropriately designed.

In that regard, this paper serves to find the optimal power limitation level for the MPPT-AAPC scheme with a target of minimizing the LCOE considering long-term mission profiles (i.e., solar irradiance and ambient temperature). In order to optimize the power limitation, a mission-profile-based analysis approach is introduced in § II, where the control and operating principle for the MPPT-AAPC scheme is also presented. As it is illustrated in § III, the obtained temperature loading profiles and power losses offer the possibility to quantitatively calculate the LCOE of the PV inverter under a given mission profile. Then, case studies on a 3-kW grid-connected PV system with the MPPT-AAPC control to optimally minimize the LCOE have been presented in § IV. Finally, concluding remarks are given in § V.

II. Absolute Active Power Control

A. Absolute Active Power Control (AAPC)

Fig. 1 shows the configuration of a double-stage single-phase grid-connected PV system with the hybrid power control and a general control structure of the boost converter stage. Although there are several AAPC possibilities to achieve a constant power generation when the available PV power, p_{pv}, exceeds the power limit, P_{limit}, a solution by modifying the
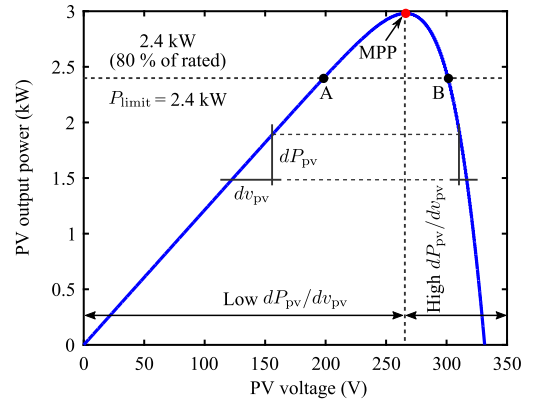
MPPT control has been adopted from the viewpoints of simplicity and cost-effectiveness [19], [34]. It can be observed in Fig. 1 that the AAPC scheme is implemented in the control of the boost converter. As mentioned previously, the PV inverter can be transformerless to maintain a high efficiency, and thus a full-bridge inverter topology with a bipolar modulation scheme is adopted in Fig. 1. Furthermore, when considering the quality of the injected grid current i_g, an *LCL* filter has been employed as the intermediate component between the full-bridge PV inverter and the grid.

In respect to the AAPC scheme employed in this paper, the operating principle of a PV system with the hybrid control scheme (MPPT-AAPC) can be described as follows. When the available PV output power p_{pv} exceeds the power limitation P_{limit}, the system should go into the AAPC mode. In that case, the PV output reference voltage v_{pv}^* is continuously "perturbed" towards certain points (e.g., points A and B as exemplified in Fig. 2), at which a constant power generation of the PV panels is achieved. While once $P_{pv} < P_{limit}$, the PV system operates in the MPPT mode with a peak power injection to the grid from the PV panels (i.e., the energy harvesting is maximized). This can further be described as

$$v_{pv}^* = \begin{cases} v_{mpp} \\ v_{mpp} \pm \Delta v \end{cases} \Rightarrow P_{pv} = \begin{cases} P_{mpp} & \text{when } p_{pv} < P_{limit} \\ P_{limit} & \text{when } p_{pv} \geq P_{limit} \end{cases}$$

(1)

where Δv is the perturbation step-size to achieve an AAPC operation, p_{pv} is the PV instantaneous (available) power, and v_{mpp} and P_{mpp} are the PV voltage and power at the Maximum Power Point (MPP). In both operational modes, a Proportional Integrator (PI) controller is employed to regulate the PV output voltage v_{pv} through controlling the boost converter, as it is shown in Fig. 1.

Fig. 3 demonstrates the performance of a 3-kW single-phase double-stage PV system with the MPPT-AAPC scheme under a trapezoidal solar irradiance profile. It can be observed in Fig. 3 that the adopted control scheme (as illustrated in Fig. 1(b) and (1)) can effectively achieve the constant power production of the PV system, as well as smooth and stable operation mode transients in contrast to the prior-art solutions [6], [16]–[18]. In this case, the PV system is operating in the region of low
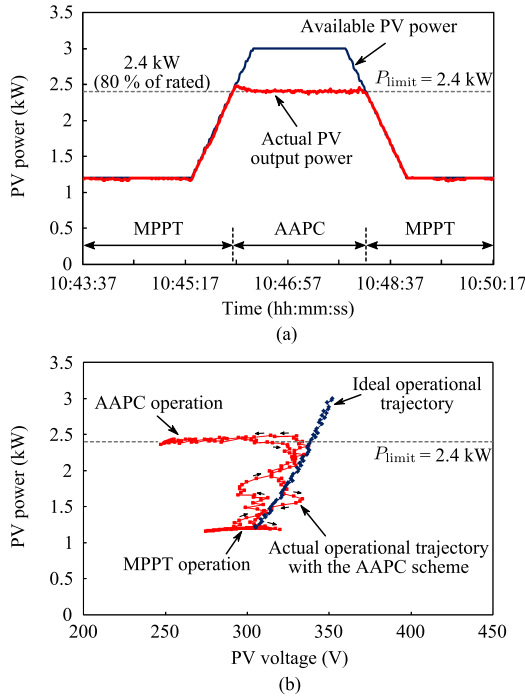
Fig. 3. Operational example (experiments) of a 3-kW single-phase double-stage PV system with the Absolute Active Power Control (AAPC) scheme, where the power limit is set to be 80 % of the rated power (i.e., $P_{\text{limit}} = 2.4$ kW) and the ambient temperature is around 25 °C: (a) PV output power and (b) operational trajectories.

$dP_{\text{pv}}/dv_{\text{pv}}$ according to the power-voltage characteristic of PV panels, as it is demonstrated in Fig. 2. That is to say, the operating point in the AAPC mode of Fig. 3 was controlled at the left-side of the MPP (i.e., point A in Fig. 2). However, it can also operate at the right-side of the MPP (i.e., point B in Fig. 2) at the cost of increased power losses (because of power variations) due to the high $dP_{\text{pv}}/dv_{\text{pv}}$ in that region [6]. Moreover, the PV system may go into instability in that case [34]. Hence, in this paper, the AAPC operating point is regulated at the left-side of the MPP, which is also enabled by the double-stage configuration (i.e., Fig. 1(a)).

B. Mission Profile Translation

A mission profile is normally referred to as a simplified representation of relevant conditions under which the considered system is operating [35]–[37]. For the grid-connected PV systems, the mission profile includes the solar irradiance and the ambient temperature of certain locations, where the PV systems were installed, and it can be taken as a reflection of the intermittent nature of the solar PV energy. Thus, the mission profile becomes an essential part for the PV inverter reliability analysis. Specifically, in order to perform the reliability analysis of the PV inverter, it is inevitable to translate the mission profile to the power losses and then the thermal loading in a long-term operation (e.g., a yearly operational profile) [31], [32], [35], [38], [39]. If not appropriately coped with, the analysis can be very time-consuming due to the process of a large amount of data. Accordingly, a time-efficient and cost-effective mission profile translation method is introduced.
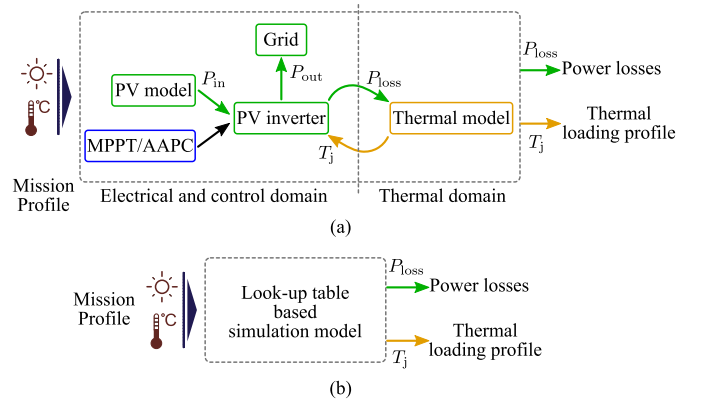

Fig. 4. An approach to translate mission profiles to power losses P_{loss} and thermal loading (i.e., device junction temperature T_{j}): (a) for short-term mission profiles and (b) for long-term mission profiles.

Fig. 4 illustrates details of the mission profile translation approach, with which the power losses and thermal loading of the power devices under any given mission profile can be obtained. Notably, a number of cases under constant environmental conditions (e.g., ambient temperature: 25 °C and solar irradiance: 1000 W/m^2) has been firstly translated according to Fig. 4(a) in order to build up the look-up table based loss and thermal models. Subsequently, a long-term mission profile even with a high sampling rate can directly be translated to the total power losses (and also energy production) as well as the thermal loading of the power devices, which are then used for LCOE analysis in the following sections.

III. LEVELIZED COST OF ENERGY OF PV INVERTERS

The PV inverter LCOE (€/Wh) is a function of the PV inverter power rating denoted as P_r [20], [27]. It can be expressed as

$$\text{LCOE}\,(P_r) = \frac{C_{\text{inv}}\,(P_r)}{E_y\,(P_r)} \tag{2}$$

in which $C_{\text{inv}}(\cdot)$ (€) is the present total cost of PV inverter during its lifetime and $E_y(\cdot)$ (Wh) is the total energy injected into the grid by the PV inverter during its life span. In the case that the PV inverter operates in the AAPC mode, its nominal power rating is constrained to $P_r = P_{\text{limit}}$ as discussed in § II.A, while in the MPPT mode it holds that $P_r = P_n$, with P_n being the inverter nominal power designed at STC – Standard Test Conditions (i.e., solar irradiance: 1 kW/m^2, solar cell temperature: 25 °C, air mass: 1.5). Namely, in the MPPT mode, the input power of the inverter is curtailed at P_n (i.e., the PV inverter is normally under-sized [40], [41]), while in the AAPC mode the power limit for curtailment is P_{limit} (i.e., to maintain a constant power production).

In (2), the present total cost of the PV inverter depends on the corresponding manufacturing and maintenance costs [27]

$$C_{\text{inv}}(P_r) = C_m(P_r) + M_c(P_r) \tag{3}$$

where $C_m(\cdot)$ (€) is the PV inverter manufacturing cost and $M_c(P_r)$ (€) is the present value of the total maintenance cost

of the PV inverter through its lifetime. Furthermore, the PV inverter manufacturing cost is proportional to P_r:

$$C_m(P_r) = c_m P_r + C_0 \qquad (4)$$

with c_m being the proportionality factor (€/kW) and C_0 being the initial cost, which has been considered as zero in this paper since it is much lower than the total cost of the PV inverter.

As a consequence, in the AAPC mode, the PV inverter cost is proportional to the pre-set power limit P_{limit}, while in the MPPT mode the inverter cost is proportional to the nominal power rating P_n that is designed at STC. The total maintenance cost, $M_c(\cdot)$, depends on the PV inverter reliability features, which in turn also depends on the power rating of the PV inverter. In the proposed methodology, the lifetime (in years) of the PV inverter power devices are initially calculated. It is assumed that each time when the end-of-life of the PV inverter power devices is reached, the maintenance of the PV inverter will be performed, imposing the corresponding maintenance cost. Therefore, the present value of the total maintenance cost of the PV inverter, $M_c(P_r)$, is calculated by reducing the (future) expenses occurring at the end of the power devices lifetime for repairing the PV inverter to the corresponding present value, as follows:

$$M_c(P_r) = \sum_{j=1}^{n} LF_j(P_r) \cdot R_c \cdot P_r \cdot \frac{(1+g)^j}{(1+d)^j} \qquad (5)$$

in which n is the PV system operational lifetime (e.g., 30 years), R_c (€/kW) is the present value of the PV inverter repairing cost per kW of the power rating, g (%) is the annual inflation rate, d (%) is the annual discount rate, and $LF_j(\cdot)$ is the inverter lifetime with $1 \leq j \leq n$. If the lifetime of the power devices expires at the j-th year of operation, $LF_j(P_n) = 1$; otherwise, $LF_j(P_n) = 0$. Notably, the repairing cost R_c in (5) consists of both the purchase cost of the failed power devices, as well as the potential labor and transportation expenses for repairing/replacing the PV inverter. The above discussion has confirmed that the AAPC control method will affect the LCOE (i.e., the cost of PV energy).

It should be pointed out that the following demonstrates how to calculate the LCOE of only the PV inverter (as shown in (2)) considering the long-term mission profile effect on the inverter lifetime, where the grid fundamental-frequency thermal cycles are not considered at this stage. However, the PV panel cost also accounts for a major share of the total cost of the entire grid-connected PV system [20], [27], where it also includes other components like capacitors and Printed Circuit Boards (PCB) for implementing the control algorithms. This becomes the main limitation of the presented LCOE optimization method, and it will affect the design results. Nevertheless, the LCOE analysis approach and also the optimization of the AAPC control power limitation can be of much value to assess and design of multiple PV systems.

IV. Minimized LCOE (Case Study Results)

A. System Description

The LCOE analysis approach has been applied for the optimal design of a PV inverter with a nominal power equal

TABLE I

PARAMETERS OF THE BP 365 SOLAR PV PANEL AT STC.

Parameter	Symbol	Value
Rated power	P_{mpp}	65 W
Voltage at P_{mpp}	V_{mpp}	17.6 V
Current at P_{mpp}	I_{mpp}	3.69 A
Open-circuit voltage	V_{oc}	21.7 V
Short-circuit current	I_{sc}	3.99 A

TABLE II

PARAMETERS OF THE SINGLE-PHASE DOUBLE-STAGE GRID-CONNECTED PV SYSTEM SHOWN IN FIG. 1.

Parameter	Symbol	Value
Grid voltage amplitude	v_{gn}	325 V
Grid frequency	ω_0	$2\pi \times 50$ rad/s
Boost converter inductor	L	5 mH
DC-link capacitor	C_{dc}	2200 μF
Grid impedance	L_g	2 mH
	R_g	0.2 Ω
LCL filter	L_1, L_2	2 mH, 3 mH
	C_{f}	4.7 μF
Sampling frequency	f_{sw}	10 kHz
Switching frequencies for both converters	f_{b}, f_{inv}	10 kHz

to $P_n = 3$ kW and also the AAPC capability. The PV system lifetime has been set to $n = 30$ years, while the financial and economic performances of the PV inverter in the AAPC and MPPT modes, respectively, have been investigated by applying the following values in (2)-(5): $c_m = 200$ €/kW, $R_c = 200$ €/kW, $g = 2$ % and $d = 5$ %. A mission profile shown in Fig. 5 with a sampling rate of 1 sample/min has been used. The BP 365 PV panel [42] is adopted in the case studies. Parameters of the PV panel are given in Table I. Three PV strings are connected in parallel to the boost converter, and each string consists of 15 PV panels in series. Thus, the rated maximum power P_{max} is around 3 kW. The other system parameters are given in Table II. Studies are then conducted according to Figs. 1 and 4. The effectiveness of the mission profile translation approach (Fig. 4) is demonstrated by the resultant thermal loading profiles presented in Fig. 6, which indicates that the junction temperature is reduced by the AAPC scheme. Hence, the PV inverter lifetime may be improved.

B. LCOE Analysis

According to the mission profile translation approach, the power losses can be obtained. Consequently, the energy yield can be calculated under different power limits P_{limit}, as it is illustrated in Fig. 7. In these simulations, the energy production has been normalized to the corresponding energy production in the MPPT mode. Due to the limitation of feed-in power in the AAPC mode, the resultant energy production shown in Fig. 7 is lower than that in the MPPT mode for $P_{\text{limit}} = 0$-110 % of the rated power P_n. However, in the case that P_{limit} is higher than 120 %, then the energy production in the AAPC mode is higher than that produced only in the MPPT mode, where the
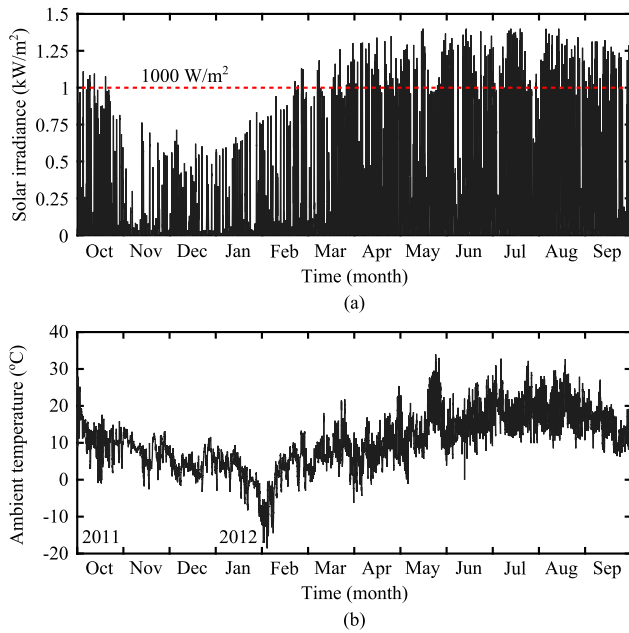
Fig. 5. A real-field yearly mission profile for a 3-kW grid-connected PV system with the absolute active power control: (a) solar irradiance and (b) ambient temperature.
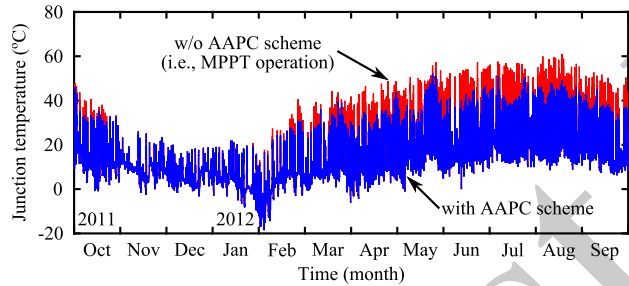

Fig. 6. Thermal loading (simulation results) of the power devices of the PV inverter with and w/o the absolute active power control (P_{limit} = 2.4 kW, i.e., 80 % of the nominal power) under the yearly mission profile (Fig. 5).

input power of the inverter is curtailed at the designed power rating P_n, as it can be observed in Fig. 7. This is because the PV panel rating has been selected to be equal to 3 kW at STC. Since the mission profile shown in Fig. 5 has some periods where the solar irradiance level is higher than 1000 W/m², the power production during those periods is higher than designed P_n, which is considered as the power limitation in the MPPT mode (i.e., the PV system is actually operating in the AAPC mode with a power limit of $P_{limit} = P_n$). Thus, during those time intervals, the excess energy is lost when even operating in the MPPT mode.

In regards to the lifetime estimation, it is not a direct outcome of the mission-profile-based analysis approach, which only gives the thermal loading profile for qualitative analysis. In order to calculate the lifetime (and then the LCOE), the thermal loading has to be "interpreted" properly according to specific lifetime models. That is to say, the information (e.g., temperature cycle amplitude and mean junction temperature) in the random loading profile should be extracted by means of a counting algorithm like a rainflow counting process [43]–
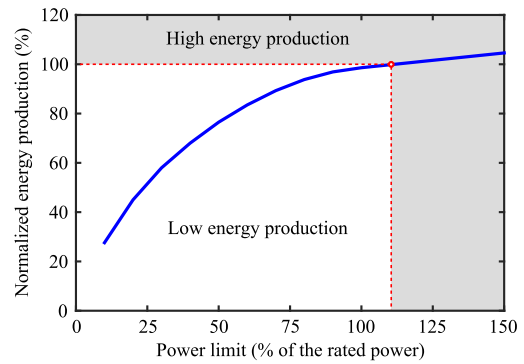

Fig. 7. Energy production (simulation results) of the 3-kW single-phase PV system in the MPPT-AAPC mode according to the mission profile shown in Fig. 5, which has been normalized to the corresponding energy production only in the MPPT mode, for various values of the power limit P_{limit}.
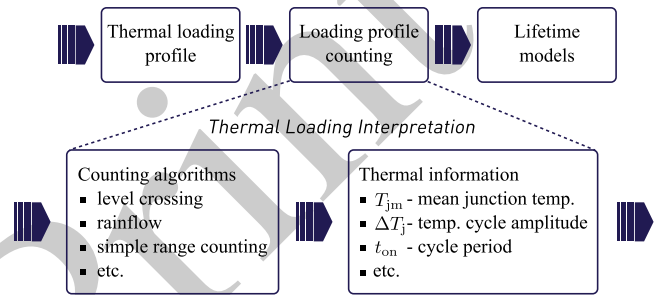

Fig. 8. Thermal loading interpretation work-flow of the loading profiles for lifetime estimation.

[45]. Fig. 8 illustrates the work-flow of "counting" the thermal loading profiles (e.g., loading profiles in Fig. 6). Then, using the extracted information, the lifetime of the power devices can be estimated according to the lifetime model [46].

Subsequently, the lifetime of the PV inverter when operating in the AAPC mode for various values of the power limitation P_{limit}, is presented in Fig. 9. It is observed in Fig. 9 that for P_{limit} = 0-100 %, the PV inverter lifetime is higher than the operational lifetime of the PV system, thus guaranteeing that no failures of the power devices will occur during that period. The corresponding present value of the lifetime maintenance cost in the AAPC mode for various values of the power limitation P_{limit}, is shown in Fig. 10. It can further be seen in Fig. 9 that, when the power limit P_{limit} reaches the range of 100-150 % of the rated power, the PV inverter lifetime in the AAPC mode is progressively reduced to around 21 years, corresponding to one repair of the PV inverter during the PV system lifetime and the maintenance cost is increased according to (5), as it is shown in Fig. 10. In contrast, according to Figs. 7 and 9, the PV inverter lifetime with the same or higher energy production is around 21 years, resulting in one inverter repair during the lifetime of the PV system, which corresponds to M_c = 326.4 €.

The total cost of the PV inverter operating in the MPPT-AAPC mode, including the manufacturing and maintenance expenses according to (3), is plotted in Fig. 11. For values of the power limit P_{limit} in the range of 0-100 % of the rated power, the maintenance cost is zero, as it is shown in Fig. 10.
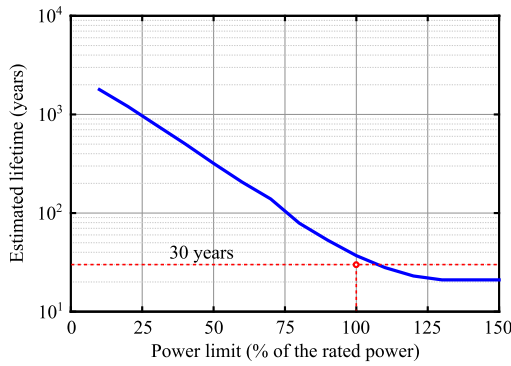
Fig. 9. Lifetime of the 3-kW single-phase PV inverter when operating in the MPPT-AAPC mode for various power limits P_{limit} considering the mission profile effect (the mission profile shown in Fig. 5 has been used).
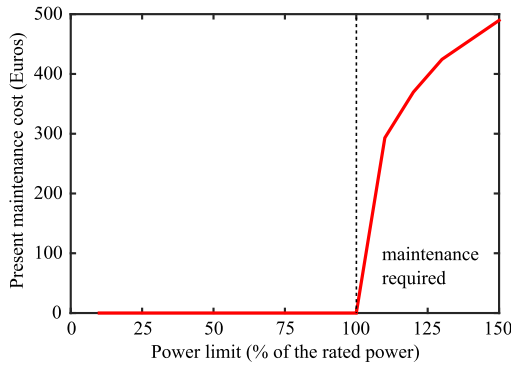

Fig. 10. Present value of the lifetime maintenance cost of the 3-kW single-phase PV inverter when operating in the MPPT-AAPC mode for various values of the power limit P_{limit}, considering the mission profile that has been presented in Fig. 5.

Fig. 11. Total cost of the 3-kW single-phase PV inverter operating in the MPPT-AAPC mode for various values of the power limit P_{limit}, where the mission profile shown in Fig. 5 has been used.

Fig. 12. LCOE of the 3-kW PV inverter system in the MPPT-AAPC mode normalized to the LCOE in the MPPT mode for various power limits P_{limit}, based on the mission profile shown in Fig. 5, where only the PV inverter is considered.

Hence, the total cost depends only on the inverter construction cost, which is proportional to the power limit P_{limit} according to (4). However, when $P_{\text{limit}} > 100$ %, the total cost in the MPPT-AAPC mode is affected by both the construction and the maintenance expenses, as indicated in Fig. 11. In the operating mode of maximum power production, the total cost of the inverter is equal to $C_{\text{inv}} = 926.4$ €. Although the lifetime energy production is higher in that case, as it is analyzed above, the PV inverter cost is also higher in this operating mode when $P_{\text{limit}} > 100\% P_n$, as shown in Fig. 11.

Moreover, the LCOE of 3-kW PV inverter in the MPPT-AAPC and MPPT modes, respectively, have been calculated using (2) for various values of the power limit P_{limit} in order to find the optimal power limitation under this mission profile shown in Fig. 5. The results are presented in Fig. 12. It can be seen in Fig. 12 that the LCOE value in the MPPT-AAPC mode is always less than that in the only-MPPT mode (i.e., the conventional operational mode at unity power factor), but the energy production is also less in the case of the MPPT-AAPC operation, as it is discussed previously.

As a consequence, it was reasonably considered that in practical applications, in order to achieve a total energy generation which is equal to or higher than that in the MPPT mode, multiple identical PV inverters would be required to operate in parallel in the MPPT-AAPC mode, each of them
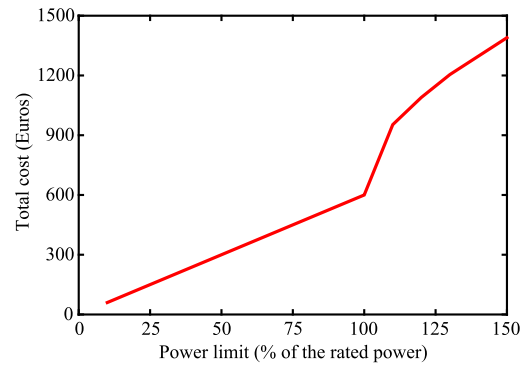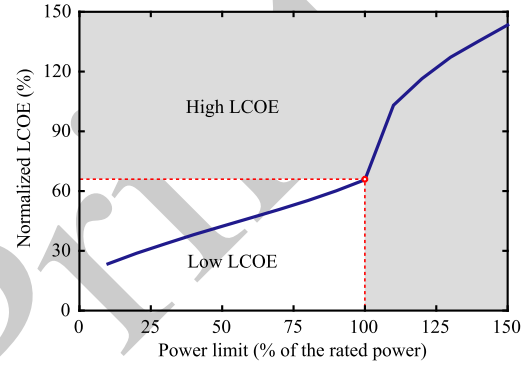
having a feed-in power limitation of P_{limit}. In this case, the total number of inverters is given by

$$N_{\text{inv}}\left(P_{\text{limit}}\right) = \left\lceil \frac{E_{\text{y, MPPT}}\left(P_n\right)}{E_{\text{y, MPPT-AAPC}}\left(P_{\text{limit}}\right)} \right\rceil \qquad (6)$$

where $N_{\text{inv}}(\cdot)$ is the number of inverters, which must operate in parallel in the MPPT-AAPC mode, $E_{\text{y, MPPT}}(\cdot)$ and $E_{\text{y, MPPT-AAPC}}(\cdot)$ are the lifetime energy productions of a single PV inverter in the MPPT and MPPT-AAPC modes, respectively. The total energy yield of the $N_{\text{inv}}(\cdot)$ PV inverters should be equal to or higher than that produced in the MPPT mode. Then, the total cost of the $N_{\text{inv}}(\cdot)$ PV inverters per unit of energy produced by each of them (denoted as $\text{LCOE}_{\text{e}}(\cdot)$) is defined as

$$\text{LCOE}_{\text{e}}\left(P_{\text{limit}}\right) = N_{\text{inv}}\left(P_{\text{limit}}\right) \cdot \text{LCOE}_{\text{MPPT-AAPC}}\left(P_{\text{limit}}\right) \quad (7)$$

with $\text{LCOE}_{\text{MPPT-AAPC}}(\cdot)$ being the LCOE of a single PV inverter operating in the MPPT-AAPC mode (see (2)). Following, the total energy production when employing $N_{\text{inv}}(\cdot)$ inverters in the MPPT-AAPC mode operating in parallel, is given by

$$E_{\text{t, MPPT-AAPC}}\left(P_{\text{limit}}\right) = N_{\text{inv}}\left(P_{\text{limit}}\right) \cdot E_{\text{y, MPPT-AAPC}}\left(P_{\text{limit}}\right) \quad (8)$$

where $E_{\text{y, MPPT-AAPC}}(\cdot)$ is the energy production of each PV inverter when operating in the MPPT-AAPC mode. Subse-

quently, the values of $\text{LCOE}_\text{e}\left(P_\text{limit}\right)$ and $E_{\text{t, MPPT-AAPC}}\left(P_\text{limit}\right)$ in (7) and (8), respectively, are normalized to the corresponding values in the MPPT mode as

$$\text{LCOE}_\text{n,e}\left(P_\text{limit}\right) = \frac{\text{LCOE}_\text{e}\left(P_\text{limit}\right)}{\text{LCOE}_\text{MPPT}\left(P_n\right)} \qquad (9)$$

and

$$E_{\text{tn, MPPT-AAPC}}\left(P_\text{limit}\right) = \frac{E_{\text{t, MPPT-AAPC}}\left(P_\text{limit}\right)}{E_{\text{y, MPPT}}\left(P_n\right)} \qquad (10)$$

with $\text{LCOE}_\text{MPPT}\left(P_n\right)$ and $E_{\text{y, MPPT}}\left(P_n\right)$ being the LCOE and the energy production of each PV inverter operating in the MPPT mode, respectively.

For various levels of the feed-in power limit, P_limit, the resultant values of $\text{LCOE}_\text{n,e}(\cdot)$, $N_\text{inv}(\cdot)$ and $E_{\text{tn, MPPT-AAPC}}(\cdot)$ are depicted in Fig. 13. The $\text{LCOE}_\text{n,e}(\cdot)$ function exhibits an overall minimum at $P_\text{limit} = 30\ \%$, which is equal to 67 %. It means that the LCOE has been minimized. In that case, by employing two identical PV inverters with a feed-in limit of $P_\text{limit} = 30\ \%$ of the rated power for each, it will result in a reduction of the total PV inverter LCOE by 33 % compared to using a single inverter unit operating only in the MPPT mode, as it can be observed in Fig. 13(b). Moreover, the total energy generated is simultaneously increased by 16 % as it is shown in Fig. 13(c). In addition, the same process with $c_m = 300\ $€/kW and $R_c = 80\ $€/kW is applied to the PV inverter under the same mission profile, and it also contributes to the minimum of $\text{LCOE}_\text{n,e}(\cdot)$ at $P_\text{limit} = 30\ \%$. In such a case, employing two inverters operating in parallel with $P_\text{limit} = 30\ \%$, the LCOE in the MPPT-AAPC mode is thus lowered by approximately 10 %, and also the total energy production is increased by 16 %, compared to the corresponding values obtained by a single PV inverter operating only in the MPPT mode.

However, as it has also been mentioned in § II, this paper only calculates the LCOE for the PV inverters, when the mission profile induced thermal cycles are considered. When the line-frequency thermal cycles are taken into account, the lifetime will be affected [14], [47]. At the same time, the LCOE in the MPPT-AAPC mode may be higher than that in the MPPT mode, if the cost of PV panels is counted in according to (3). In that case, it is still possible to derive the optimal PV system configurations by mixing a low power PV inverter with a higher power one, both operating in the MPPT-AAPC mode, according to the presented optimization method. Similar objectives (minimized LCOE and maximized energy production) can then be reached.

Alternatively, in practice, the PV panels are already available in a pre-designed system (e.g., 3-kW), and according to the optimization analysis presented in this paper (i.e., Fig. 13), it is better to split the PV panels into two arrays and install two inverters of 1 kW (i.e., approx. 30 % of the pre-designed 3-kW system) operating in the MPPT-AAPC. In such a case, although the cost of the PV modules is not considered in the analysis in the paper, which should be paid for both the 3-kW system in MPPT mode and the two 1-kW systems in the MPPT-AAPC mode, the investigation in this paper is valid in terms of minimized LCOE while maintaining a higher energy production.
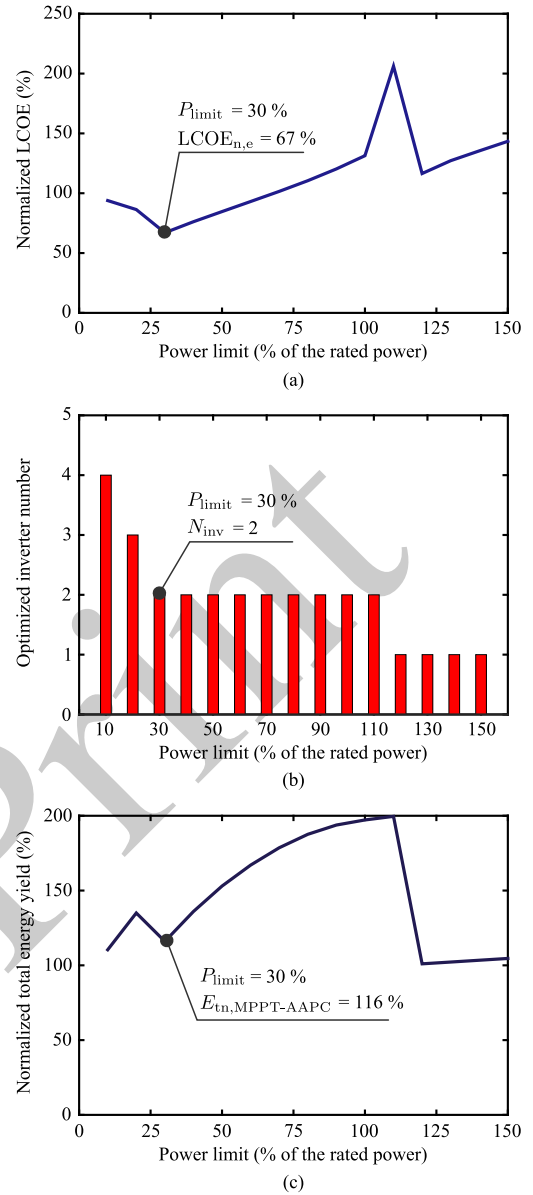

Fig. 13. Optimized results for the 3-kW PV inverter systems with the MPPT-AAPC scheme for various levels of the feed-in power limit P_limit when only considering the cost of the PV inverters: (a) minimized $\text{LCOE}_\text{n, e}(\cdot)$, (b) optimized number of PV inverters in parallel N_inv, and (c) obtained total energy production $E_{\text{tn, MPPT-AAPC}}(\cdot)$.

V. CONCLUSION

The Levelized Cost Of Energy (LCOE) of PV inverters with an Absolute Active Power Control (AAPC) scheme has been calculated and analyzed in this paper in the consideration of a long-term real-field mission profile. The analysis has revealed that the hybrid power control (i.e., with the mixture of MPPT and AAPC operational modes, MPPT-AAPC) can contribute to an improved lifetime of the power devices due to the reduced thermal loading. However, a reduction of energy production is associated with this reliability benefit, when the hybrid active power control scheme is enabled. In this paper, it has been demonstrated that by optimizing the power limit imposed on multiple PV inverters, which operate in the hybrid MPPT-AAPC mode, a reduction of LCOE (minimized) can

be obtained. Simultaneously, an increase of the PV generated energy is achieved, compared to the use of a single PV inverter, which operates only in the MPPT mode.

Most importantly, the presented optimization method and the LCOE analysis can be an effective design tool for PV system planning (e.g., a cluster of PV inverters), when the mission profile (both long-term and line-frequency thermal cycles) and the PV panel cost are also considered. Specifically, by applying the last part of the optimization design in this paper (i.e., related to Fig. 13), the operation of each individual inverter in the cluster of the PV systems can be optimally selected, in such a way that:

1) an overall constant power production is achieved,
2) the total energy production is not reduced, and
3) the LCOE is minimized.

REFERENCES

[1] SolarPower Europe, "Global market outlook for solar power 2015 - 2019," Euoropean Photovoltaic Industry Association, Bruxelles, Tech. Rep., 2015. [Online]. Available: http://www.solarpowereurope.org/

[2] D. Rosenwirth and K. Strubbe, "Integrating variable renewables as Germany expands its grid," *RenewableEnergyWorld.com*, Mar. 21, 2013. [Online]. Available: http://www.renewableenergyworld.com

[3] Fraunhofer ISE, "Recent facts about photovoltaics in Germany," Fraunhofer Institute for Solar Energy Systems ISE, Germany, Tech. Rep., 25 Dec. 2015. [Online]. Available: https://www.ise.fraunhofer.de/en/renewable-energy-data/renewable-energy-data

[4] E. Reiter, K. Ardani, R. Margolis, and R. Edge, "Industry perspectives on advanced inverters for U.S. solar photovoltaic systems: benefits, deployment challenges, and emerging solutions," National Renewable Energy Laboratory (NREL), USA, Tech. Rep., Sept. 2015. [Online]. Available: http://www.nrel.gov/docs/fy15osti/65063.pdf

[5] Y. Yang, P. Enjeti, F. Blaabjerg, and H. Wang, "Wide-scale adoption of photovoltaic energy: Grid code modifications are explored in the distribution grid," *IEEE Ind. Appl. Mag.*, vol. 21, no. 5, pp. 21–31, Sept. 2015.

[6] Y. Yang, H. Wang, F. Blaabjerg, and T. Kerekes, "A hybrid power control concept for PV inverters with reduced thermal loading," *IEEE Trans. Power Electron.*, vol. 29, no. 12, pp. 6271–6275, Dec. 2014.

[7] ENERGINET.DK, "Pv power plants with a power output above 11 kW," *Technical Regulation 3.2.2 (2nd Edition)*, Mar. 2015.

[8] ENERGINET.DK, "Wind power plants with a power output greater than 11 kW," *Technical Regulation 3.2.5*, Sept. 2010.

[9] "German federal law: Renewable energy sources act (gesetz fur den vorrang erneuerbarer energien)," *Std.*, Jul. 2014.

[10] M. Lang and A. Lang, "The 2014 German renewable energy sources act revision–from feed-in tariffs to direct marketing to competitive bidding," *Journal of Energy & Natural Resources Law*, vol. 33, no. 2, pp. 131–146, 2015.

[11] H. Kobayashi, "Grid interconnection requirements and techniques for distributed power generation in Japan," in *Proc. of WECC*, 28 Nov. - 4 Dec. 2015.

[12] T. Stetz, F. Marten, and M. Braun, "Improved low voltage grid-integration of photovoltaic systems in Germany," *IEEE Trans. Sustain. Energy*, vol. 4, no. 2, pp. 534–542, Apr. 2013.

[13] H. Beltran, E. Perez, N. Aparicio, and P. Rodriguez, "Daily solar energy estimation for minimizing energy storage requirements in PV power plants," *IEEE Trans. Sustain. Energy*, vol. 4, no. 2, pp. 474–481, Apr. 2013.

[14] Y. Yang, H. Wang, and F. Blaabjerg, "Improved reliability of single-phase PV inverters by limiting the maximum feed-in power," in *Proc. of ECCE*, pp. 128–135, Sept. 2014.

[15] H. Beltran, E. Bilbao, E. Belenguer, I. Etxeberria-Otadui, and P. Rodriguez, "Evaluation of storage energy requirements for constant production in PV power plants," *IEEE Trans. Ind. Electron.*, vol. 60, no. 3, pp. 1225–1234, Mar. 2013.

[16] A. Sangwongwanich, Y. Yang, and F. Blaabjerg, "High-performance constant power generation in grid-connected PV systems," *IEEE Trans. Power Electron.*, vol. 31, no. 3, pp. 1822–1825, Mar. 2016.

[17] A. Ahmed, L. Ran, S. Moon, and J.-H. Park, "A fast PV power tracking control algorithm with reduced power mode," *IEEE Trans. Energy Convers.*, vol. 28, no. 3, pp. 565–575, Sept. 2013.

[18] A. Hoke and D. Maksimovic, "Active power control of photovoltaic power systems," in *Proc. of SusTech*, pp. 70–77, Aug. 2013.

[19] J. von Appen, A. Hettrich, and M. Braun, "Grid planning and operation with increasing amounts of PV storage systems," *presented at IRES*, 10 Mar. 2015.

[20] Fraunhofer ISE, "Levelized cost of electricity-renewable energy technologies," Fraunhofer Institute for Solar Energy Systems ISE, Freiburg, Germany, Tech. Rep., Nov. 2013. [Online]. Available: http://www.ise.fraunhofer.de

[21] Y. Xue, K.C. Divya, G. Griepentrog, M. Liviu, S. Suresh, and M. Manjrekar, "Towards next generation photovoltaic inverters," in *Proc. of ECCE*, pp. 2467–2474, Sept. 2011.

[22] J.-Y. Chen, C.-H. Hung, J. Gilmore, J. Roesch, and W. Zhu, "LCOE reduction for megawatts PV system using efficient 500 kW transformerless inverter," in *Proc. of ECCE*, pp. 392–397, Sept. 2010.

[23] R. Fu, T. L. James, and M. Woodhouse, "Economic measurements of polysilicon for the photovoltaic industry: market competition and manufacturing competitiveness," *IEEE J. Photovoltaics*, vol. 5, no. 2, pp. 515–524, Mar. 2015.

[24] J. N. Mayer, P. Simon, N. S. H. Philipps, T. Schlegl, and C. Senkpiel, "Current and future cost of photovoltaics," *presented at the IRENA Cost Competitiveness Workshop, Bonn, Germany (Fraunhofer ISE, Study on behalf of Agora Energiewende)*, 23 Mar. 2015.

[25] Y. Yang, E. Koutroulis, A. Sangwongwanich, and F. Blaabjerg, "Minimizing the levelized cost of energy in single-phase photovoltaic systems with an absolute active power control," in *Proc. of ECCE*, pp. 28–34, Sept. 2015.

[26] Department of Defense, US Military, "Reliability prediction of electronic equipment," MIL-HDBK-217F Notice 1, Tech. Rep., 1992.

[27] E. Koutroulis and F. Blaabjerg, "Design optimization of transformerless grid-connected PV inverters including reliability," *IEEE Trans. Power Electron.*, vol. 28, no. 1, pp. 325–335, Jan. 2013.

[28] S. Saridakis, E. Koutroulis, and F. Blaabjerg, "Optimization of SiC-based H5 and Conergy-NPC transformerless PV inverters," *IEEE J. Emerg. Sel. Top. Power Electron.*, vol. 3, no. 2, pp. 555–567, Jun. 2015.

[29] Z. Moradi-Shahrbabak, A. Tabesh, and G.R. Yousefi, "Economical design of utility-scale photovoltaic power plants with optimum availability," *IEEE Trans. Ind. Electron.*, vol. 61, no. 7, pp. 3399–3406, Jul. 2014.

[30] H. Wang, M. Liserre, F. Blaabjerg, P. de Place Rimmen, J.B. Jacobsen, T. Kvisgaard, and J. Landkildehus, "Transitioning to physics-of-failure as a reliability driver in power electronics," *IEEE J. Emerg. Sel. Top. Power Electron.*, vol. 2, no. 1, pp. 97–114, Mar. 2014.

[31] P. Diaz Reigosa, H. Wang, Y. Yang, and F. Blaabjerg, "Prediction of bond wire fatigue of igbts in a pv inverter under a long-term operation," *IEEE Trans. Power Electron.*, vol. PP, no. 99, pp. 1–12, DOI: 10.1109/TPEL.2015.2509643, in press, 2015.

[32] Y. Yang, H. Wang, F. Blaabjerg, and K. Ma, "Mission profile based multi-disciplinary analysis of power modules in single-phase transformerless photovoltaic inverters," in *Proc. of EPE*, pp. 1–10, Sept. 2013.

[33] T. K. S. Freddy, N. A. Rahim, W.-P. Hew, and H. S. Che, "Comparison and analysis of single-phase transformerless grid-connected pv inverters," *IEEE Trans. Power Electron.*, vol. 29, no. 10, pp. 5358–5369, Oct. 2014.

[34] A. Sangwongwanich, Y. Yang, F. Blaabjerg, and H. Wang, "Benchmarking of constant power generation strategies for single-phase grid-connected photovoltaic systems," in *Proc. of APEC*, pp. 370–377, Mar. 2016.

[35] D. Hirschmann, D. Tissen, S. Schroder, and R.W. De Doncker, "Reliability prediction for inverters in hybrid electrical vehicles," *IEEE Trans. Power Electron.*, vol. 22, no. 6, pp. 2511–2517, Nov. 2007.

[36] M. Ciappa, "Lifetime prediction on the base of mission profiles," *Microelectronics reliability*, vol. 45, no. 9, pp. 1293–1298, 2005.

[37] S.E. De Leon-Aldaco, H. Calleja, and J. Aguayo Alquicira, "Reliability and mission profiles of photovoltaic systems: a FIDES approach," *IEEE Trans. Power Electron.*, vol. 30, no. 5, pp. 2578–2586, May 2015.

[38] M. Musallam, C. Yin, C. Bailey, and M. Johnson, "Mission profile-based reliability design and real-time life consumption estimation in power electronics," *IEEE Trans. Power Electron.*, vol. 30, no. 5, pp. 2601–2613, May 2015.

[39] S.E. de León-Aldaco, H. Calleja, F. Chan, and H.R. Jiménez-Grajales, "Effect of the mission profile on the reliability of a power converter aimed at photovoltaic applications - a case study," *IEEE Trans. Power Electron.*, vol. 28, no. 6, pp. 2998–3007, Jun. 2013.

[40] B. Burger and R. Rüther, "Inverter sizing of grid-connected photovoltaic systems in the light of local solar resource distribution characteristics and temperature," *Solar Energy*, vol. 80, no. 1, pp. 32–45, 2006.

[41] S. Chen, P. Li, D. Brady, and B. Lehman, "Optimum inverter sizing in consideration of irradiance pattern and PV incentives," in *Proc. of APEC*, pp. 982–988, Mar. 2011.

[42] Plexim GmbH, "PLECS User Manual Version 3.6," 14 Nov. 2014. [Online]. Available: http://www.plexim.com

[43] M. Musallam and C.M. Johnson, "An efficient implementation of the rainflow counting algorithm for life consumption estimation," *IEEE Trans. Reliability*, vol. 61, no. 4, pp. 978–986, Dec. 2012.

[44] A.T. Bryant, P.A. Mawby, P.R. Palmer, E. Santi, and J.L. Hudgins, "Exploration of power device reliability using compact device models and fast electrothermal simulation," *IEEE Trans. Ind. Appl.*, vol. 44, no. 3, pp. 894–903, May 2008.

[45] H. Huang and P.A. Mawby, "A lifetime estimation technique for voltage source inverters," *IEEE Trans. Power Electron.*, vol. 28, no. 8, pp. 4113–4119, Aug. 2013.

[46] U. Scheuermann, "Pragmatic bond wire model," *presentation at ECPE Workshop Lifetime Modeling Simulation*, Jul. 2013.

[47] K. Ma, M. Liserre, F. Blaabjerg, and T. Kerekes, "Thermal loading and lifetime estimation for power device considering mission profiles in wind power converter," *IEEE Trans. Power Electron.*, vol. 30, no. 2, pp. 590–602, Feb. 2015.

Eftichios Koutroulis (M'10-SM'15) was born in Chania, Greece, in 1973. He received his B.Sc., M.Sc. and Ph.D. degrees in the School of Electronic and Computer Engineering of the Technical University of Crete (Chania, Greece) in 1996, 1999 and 2002, respectively.

He is currently an Assistant Professor at the School of Electronic and Computer Engineering of the Technical University of Crete. His research interests include power electronics, energy harvesting, the development of microelectronic energy management systems for RES and the design of photovoltaic and wind energy conversion systems.

Ariya Sangwongwanich was born in Bangkok, Thailand, in 1991. He received the B.Eng degree in electrical engineering from Chulalongkorn University, Thailand, in 2013, and the M.Sc. in energy engineering from Aalborg University, Denmark, in 2015, where he is currently working as a research assistant. His research interests include control of grid-connected converter, photovoltaic system, and high-power multilevel converter.

Yongheng Yang (S'12-M'15) received the B.Eng. degree from Northwestern Polytechnical University, China, in 2009, and the Ph.D. degree from Aalborg University, Denmark, in 2014.

He was a Post-Graduate with Southeast University, China, from 2009 to 2011. In 2013, he was a Visiting Scholar with the Department of Electrical and Computer Engineering, Texas A&M University, USA. Since 2014, he has been with the Department of Energy Technology, Aalborg University, where he is currently an Assistant Professor. His research interests are focused on grid integration of renewable energy systems, power converters design and control, harmonics identification and mitigation, and the reliability of power electronics.

Dr. Yang is involved in the IEEE Industry Applications Society student activities. He is a Member of the IEEE Power Electronics Society Young Professionals Committee. He serves as a Guest Associate Editor of the IEEE JOURNAL OF EMERGING AND SELECTED TOPICS IN POWER ELECTRONICS special issue on Power Electronics for Energy Efficient Buildings.

Frede Blaabjerg (S'86-M'88-SM'97-F'03) was with ABB-Scandia, Randers, Denmark, from 1987 to 1988. From 1988 to 1992, he was a Ph.D. Student with Aalborg University, Aalborg, Denmark. He became an Assistant Professor in 1992, Associate Professor in 1996, and Full Professor of power electronics and drives in 1998. His current research interests include power electronics and its applications such as in wind turbines, PV systems, reliability, harmonics and adjustable speed drives.

He has received 17 IEEE Prize Paper Awards, the IEEE PELS Distinguished Service Award in 2009, the EPE-PEMC Council Award in 2010, the IEEE William E. Newell Power Electronics Award 2014 and the Villum Kann Rasmussen Research Award 2014. He was an Editor-in-Chief of the IEEE TRANSACTIONS ON POWER ELECTRONICS from 2006 to 2012. He is nominated in 2014 and 2015 by Thomson Reuters to be between the most 250 cited researchers in Engineering in the world.